JOURNAL OF AGRICULTURAL AND FOOD CHEMISTRY

Article

pubs.acs.org/JAFC

Improved Physical and in Vitro Digestion Stability of a Polyelectrolyte Delivery System Based on Layer-by-Layer Self-Assembly Alginate–Chitosan-Coated Nanoliposomes

Weilin Liu,[†] Jianhua Liu,[‡] Wei Liu,*[,†] Ti Li,[†] and Chengmei Liu*[,†]

[†]State Key Laboratory of Food Science and Technology, Nanchang University, Nanchang 330047, Jiangxi, People's Republic of China

[‡]College of Biological and Environmental Engineering, Zhejiang University of Technology, Hangzhou 310014, Zhejiang, People's Republic of China

ABSTRACT: To improve lipid membrane stability and prevent leakage of encapsulated food ingredients, a polyelectrolyte delivery system (PDS) based on sodium alginate (AL) and chitosan (CH) coated on the surface of nanoliposomes (NLs) has been prepared and optimized using a layer-by-layer self-assembly deposition technique. Morphology and FTIR observation confirmed PDS has been successfully coated by polymers. Physical stability studies (pH and heat treatment) indicated that the outer-layer polymers could protect the core (NLs) from damage, and PDS showed more intact structure than NLs. Further enzymic digestion stability studies (particle size, surface charge, free fatty acid, and model functional component release) demonstrated that PDS could better resist lipolytic degradation and facilitate a lower level of encapsulated component release in simulated gastrointestinal conditions. This work suggested that deposition of polyelectrolyte on the surface of NLs can stabilize liposomal structure, and PDS could be developed as a formulation for delivering functional food ingredients in the gastrointestinal tract.

KEYWORDS: *nanoliposomes, polyelectrolyte delivery system, stability, self-assembly, digestion, release kinetics*

INTRODUCTION

A liposome, in which a lipid bilayer encapsulates a fraction of the surrounding aqueous medium, is one of the most extensively investigated delivery system.[1] It has been orally used in food, pharmaceutic, and agricultural industries to entrap, protect, and control the release of functional and unstable hydrophilic or lipophilic compounds, such as enzymes, antimicrobials, vaccines, and antioxidants.[2−5] To date, however, the practical applications of liposomes have been limited by their insufficient physical stability and digested stability in the gastrointestinal tract, with disruption of liposome integrity and leakage of the encapsulated molecule.[6] The environment conditions, including the pH, temperature, and enzyme, can readily cause liposomes to change their particle diameter, damage structural integrity, and leak the entrapped ingredients.[7,8] To improve liposomal stability, a variety of surface-modified systems have been developed, for example, poly(ethylene glycol)-surface-conjugated liposomes,[9] chitosan-coated liposomes,[10] silica external-layered liposomes,[11] and protein site-specific modified liposomes.[12]

Chitosan (CH) is a biocompatible cationic polysaccharide with low toxicity. Several studies have highlighted the potential use of CH as a stability-enhancing agent and bioadhesive material by coating on the liposomal surface.[13,14] However, the main limitation of CH as a carrier is its easy dissolution in the low pH of the stomach, resulting in the encapsulated ingredient being denatured.[15] Alginate (AL), a water-soluble anionic polymer, is used extensively as a thickener, emulsifier, and stabilizer.[16] Although AL can be layered on the external membrane of liposomes for delivery purposes,[17] its major drawback is its dissolution in high-pH conditions and the subsequent loss of its protection effect and the release of the entrapped contents.

In view of these limitations of CH and AL, the concept of AL−CH polyelectrolyte layer-by-layer (LbL) self-assembly surface coating technique has gained acceptance in recent years. Such assembly is believed to be driven by electrostatic attraction and complex formation between polyanions and polycations.[18] Complexation of CH with AL can reduce the porosity of AL and decrease the leakage of the encapsulated ingredients more effectively than either AL or CH alone.[19] Ye et al.[20] prepared microcrystals using CH and AL and found the indomethacin could better control release than the uncoated. Zhao et al.[21] reported a colloidal particle obtained from AL−CH onto carboxylmethylcellulose-doped $CaCO_3$, and their results showed that the encapsulated doxorubicin had an improved tumor inhibition. Besides, Haidar et al.[22] have constructed through the LbL self-assembly method a multilayered core (liposome)−shell (AL−CH) delivery system for decreasing the leakage of the encapsulated protein. However, the digestion stability of AL−CH-coated liposomes in the gastrointestinal tract is unknown, and the physical stability of these polyelectrolyte particles needs to be further discussed as well.

Various nanoliposomes (NLs) had been prepared to encapsulate hydrophilic and hydrophobic nutrients by different methods in our laboratory, such as medium-chain fatty acids

Received: December 13, 2012
Revised: April 1, 2013
Accepted: April 9, 2013
Published: April 9, 2013

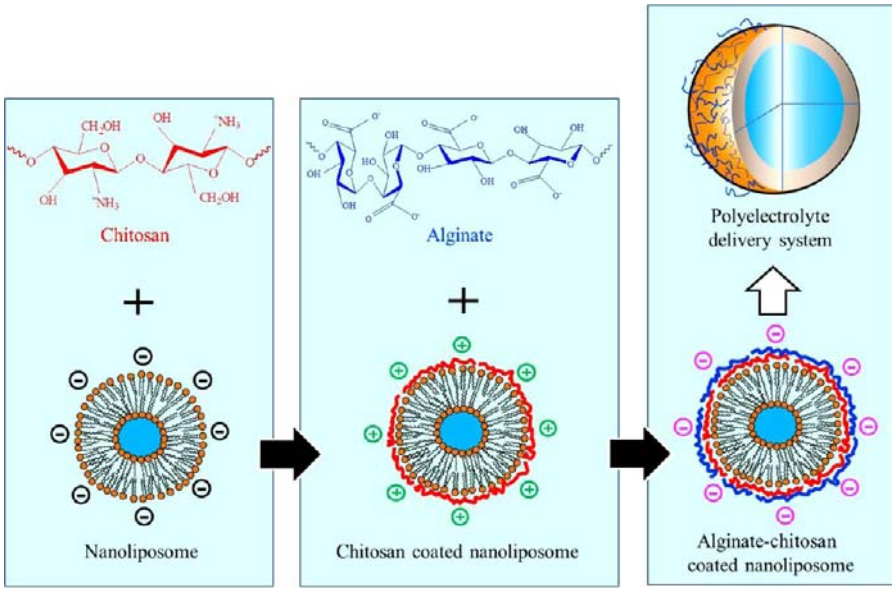

Figure 1. Preparation of polyelectrolyte delivery system by layer-by-layer (LbL) self-assembly of chitosan and alginate onto a nanoliposome.

(MCFAs) NLs for suppressing body fat accumulation and Vc NLs as a vitamin supplement.[23−26] Nevertheless, no information related to the improvement of stability by surface coating was involved. Thus, the aim of the present study was to combine the advantages of NLs with those of LbL self-assembly systems to develop a polyelectrolyte delivery system (PDS) that was composed of liposomes coated by CH and AL. As shown in Figure 1, positively charged CH was self-assembly coated on the surface of anionic liposomes, and negatively charged AL was then deposited on the outer layer of cationic liposomes; the CH−AL-stabilized liposome was the PDS. The delivery system was then characterized using dynamic light scattering (DLS), atomic force microscopy (AFM), and Fourier transform infrared spectroscopy (FTIR). The major focus of this paper was on the effect of pH and heat treatment on the physical stability of PDS. In addition, the digestion stability including particle size, zeta potential, and free fatty acid (FFA) release was also evaluated. A hydrophobic model functional ingredient, MCFAs, was entrapped in PDS to assess the release kinetics under in vitro simulated gastrointestinal conditions.

EXPERIMENTAL PROCEDURES

Materials. L-α-Phosphatidylcholine from soybean (P3644, Sigma-Aldrich Chemical Co., St. Louis, MO, USA) contained ≥30% phosphatidylcholine, polar lipids ≥73%, and saturated fatty acids ≥20 wt %. Chitosan (CH; 448869, viscosity < 50 mps, 50 kDa) and sodium alginate (AL; A0682, low viscosity, 12 kDa) were obtained from Sigma-Aldrich. MCFAs were kindly provided by UPMC (Pittsburgh, PA, USA). Pepsin from porcine gastric mucosa (P7000, enzymatic activity of 800−2500 units/mg protein), pancreatin from porcine pancreas (P1750, 4× U.S. Pharmacopeial (USP) specifications), and bile extract porcine (B8631) were purchased from Sigma-Aldrich. A Pi kit and a malondialdehyde (MDA) kit were purchased from Nanjing Jiancheng Bioengineering Institute (Nanjing, China). All other chemicals used were of analytical grade.

Formulation of NLs. A thin layer dispersion method combined with dynamic high-pressure microfluidization (DHPM) was used to prepare NLs as described in our previous study.[23] Briefly, soybean phospholipids, cholesterol, Tween-80, and vitamin E were mixed in a mass ratio of 6:1:1.8:0.12. The mixture was well dissolved in absolute ethanol and then evaporated to a thin film under vacuum at 55 °C. The dried lipid film was rehydrated with phosphate-buffered saline (PBS; pH 7.4, 0.05 M) to prepare a crude liposome suspension. To obtain NLs, DHPM treatment was carried out continuously with a microfluidizer (M-110EH30, Microfluidic Corp., Newton, MA, USA), which works on the principle of dividing a pressurized stream into two parts, passing each part through a fine orifice, and impacting or colliding the parts against each other in the interaction chamber,[27] at a pressure of 120 MPa and for two cycles. The final concentration of the lipid (phospholipid and cholesterol) was about 8 mg/mL. In addition, NL-encapsulated MCFAs (1.28 mg/mL) were prepared using the same procedures by mixing MCFAs with the lipid phase.

Preparation of PDS. Fresh CH solutions were prepared by dissolving CH in 1% glacial acetic acid aqueous solution at concentrations of 0.05, 0.2, 0.6, 1, and 2%, respectively. Sodium AL solutions (0.1, 0.3, 0.5, 1, and 2%, respectively) were prepared in Milli-Q water. Both of the solutions were stirred overnight and adjusted to pH 5.5 followed by filtration.

PDS based on CH−AL deposition on the surface of NLs was LbL self-assembled in two steps. The first layer was deposited by addition of NLs into CH solution (1:1, v/v) and then incubated for 1 h under gentle stirring. The subsequent AL layer was deposited by dropping CH−NLs into the AL solution (1:1, v/v) using the same procedure. The obtained AL−CH-coated liposomes were adjusted to pH 5.5 with centrifugation at 3000*g* following for 15 min to eliminate aggregation. The concentrations of CH and AL were optimized by the parameters of average diameter, polydispersion index (PDI), zeta potential, coating efficiency, and sedimentation efficiency, respectively. The coating efficiency and sedimentation efficiency were measured according to the methods of Guo et al.[28] and Zhang et al.[29] with slight modification, respectively. Briefly, CH−NLs were centrifugated at 15000*g* for 30 min. Then the phosphor content within the sedimentation was determined with the Pi kit. The total content of phosphor was measured by using the same method without centrifugation. The coating efficiency was calculated from eq 1. For the sedimentation efficiency measurement, PDS was centrifugated at 3000*g* for 15 min, and the sedimentation was weighed after removal of the supernatant. The sedimentation efficiency was calculated from eq 2.

$$\text{coating efficiency } \% = \frac{\text{Pi}_{(\text{in})}}{\text{Pi}_{(\text{total})}} \quad (1)$$

$\text{Pi}_{(\text{in})}$ is the phosphor content within the CH−NLs and $\text{Pi}_{(\text{total})}$ is the total phosphor content of liposomes.

Table 1. Optimization of the Concentrations of Chitosan (CH) and Sodium Alginate (AL) for Preparation of a Polyelectrolyte Delivery System (PDS)[a]

sample			av diameter (nm)	PDI	zeta potential (mV)	coating efficiency (%)	sedimentation efficiency (%)
NLs			89.3 ± 11.8	0.26 ± 0.05	−6.34 ± 0.62		
CH-coated NLs	CH concn (%, w/v)	0.05	124.6 ± 18.9	0.28 ± 0.02	−1.15 ± 0.46	64.0 ± 3.2	
		0.2	135.7 ± 10.5	0.26 ± 0.09	1.23 ± 0.31	65.1 ± 5.4	
		0.6	**160.3 ± 28.3**	**0.26 ± 0.11**	**2.27 ± 0.67**	**65.3 ± 4.1**	
		1	182.2 ± 3.2	0.30 ± 0.07	2.99 ± 0.58	65.7 ± 3.8	
		2	255.8 ± 34.8	0.36 ± 0.12	3.18 ± 0.28	68.2 ± 6.6	
PDS	AL concn (%, w/v)	0.1	170.5 ± 28.1	0.29 ± 0.05	1.51 ± 0.37		6.6 ± 1.9
		0.3	211.1 ± 6.1	0.32 ± 0.06	−4.79 ± 0.26		10.4 ± 0.4
		0.5	**330.6 ± 37.3**	**0.37 ± 0.12**	**−15.79 ± 0.70**		**19.5 ± 1.1**
		1	1170.3 ± 404.5	0.59 ± 0.07	−15.81 ± 0.61		24.8 ± 0.8
		2	3229.7 ± 203.4	0.80 ± 0.16	−16.10 ± 0.34		21.4 ± 2.5

[a]Data are expressed as the mean ± SD.

$$\text{sedimentation efficiency \%} = \frac{W_s}{W_0} \quad (2)$$

W_s is the weight of sedimentation and W_0 is the total weight of PDS before centrifugation.

Characterization of PDS. The average diameter and surface charge of NLs and PDS were measured at 25 °C using a DLS instrument (Nicomp 380 ZLS, Santa Barbara, CA, USA). The intensity was detected at an angle of 90°. NLs and PDS were diluted 10- and 2.5-fold in PBS, respectively. All data were calculated as the average of at least triplicate measurements. Morphological analysis was performed by AFM and TEM, respectively. For AFM, the samples were prepared by drying a drop of suspension on a freshly cleaved mica substrate, and images of samples were acquired using an AFM (Agilent 5500, Agilent Technologies, Santa Clara, CA, USA) with a silicon cantilever of force constant of 0.58 N m^{1-} in tapping mode at room temperature. For TEM, a copper mesh grid was placed onto droplets of a sample solution, which was diluted to a phospholipid concentration of 1 mg/mL with distilled water. After 4 min, the grid was stained with uranyl acetate solution (2%) for 4 min and air-dried at room temperature after excess liquid had been removed with filter paper. The grid with sample was examined under a TEM (Tecnai G2 Spirit, JEOL) at a voltage of 120 kV. Infrared spectra of the samples was observed with a spectrophotometer (Nicolet 5700, Thermo Electron Co., Waltham, MA, USA) by the KBr tablet method at a resolution of 0.09 cm^{-1} and a scan rate of 65 times per second, over the range of 4000−400 cm^{-1}.

Physical Stability. The influence of pH on the stability of NLs and PDS was determined by preparing a series of samples with aqueous phases adjusted to values ranging from pH 1.5 to 9 using either HCl or NaOH. The changes in particle size and zeta potential were assessed by the DLS instrument mentioned above.

Heat treatment was carried out by placing liposomes in a water bath at 70 °C for 48 h. Heated samples were taken out at different time intervals (0, 1, 6, 12, 24, 36, and 48 h) and then rapidly cooled to room temperature for analysis. Except for size distribution and surface charge, appearance, color difference, and malondialdehyde (MDA) changes of liposomes were recorded as well. For color difference analysis, the *L*, *a*, and *b* coordinates of the samples were determined using a light reflectance spectrophotometer (CM-3600D, Minolta), as compared with PBS. The color differences (DE) of the sample before and after heat treatment were calculated using the following equation:

$$\text{DE} = \sqrt{\Delta L^2 + \Delta a^2 + \Delta b^2} \quad (3)$$

MDA, a final product of fatty acid peroxidation, reacted with thiobarbituric acid to form a colored complex that had a maximum spectrophotometrical absorbance at 532 nm. MDA values were expressed according to the recommended procedures provided by the kit.

Digestion Stability. In vitro digestion of the samples was carried out in simulated gastric fluid (SGF) and simulated intestinal fluid (SIF) separately according to our previous study with slight modification.[30] Briefly, NLs were mixed with SGF containing pepsin (3.2 mg/mL) or SIF containing pancreatin (3.2 mg/mL) with a volume ratio of 1:4, whereas PDS was diluted with SGF or SIF in the ratio of 4:1 (v/v). The resultant mixture was then incubated in a shaking water bath (95 rpm) at 37 °C, and subsamples were taken for average diameter and zeta potential analysis at various time intervals (0, 1, 5, 15, 30, 60, and 120 min). Particularly, SGF and SIF were prepared as described in Singh et al.,[31] with the bile salts concentration of 0.2 mg/mL in SIF. Before in vitro liposome digestion, the SGF and SIF were incubated at 37 °C for preheating in the water bath. The pH and the temperature were continuously monitored and controlled.

In vitro lipid digestion was measured by determining the release of free fatty acid (FFA) from liposomal phospholipids using a titration method, similar to that described by Bonnaire et al.[32] The phospholipid concentrations of NLs and PDS before digestion were calibrated using the Pi kit method (as described in the previous paragraph).[33] NLs and PDS were mixed with SIF in a volume ratio of 1:4 and 4:1, respectively, and the pH was adjusted to 7.4, prior to heating to 37 °C. The amount of FFA released after the addition of pancreatin (3.2 mg/mL) was determined by direct titration with 0.05 M NaOH using a buret to reach an end point of pH 7.4. The FFA release rate was reported as the percentage of FFA released compared to the total amount that would be released if all of the triacylglycerol molecules present were converted to one monoacylglycerol and two FFA molecules. A standard curve was constructed using the same titration method to measure the FFA present in liposomes and SIF (1:3, v/v) with known concentrations (0−15000 μmol) of oleic acid.

The release kinetics of MCFAs from NLs and PDS into the surrounding medium was measured at 37 °C. After digestion in SGF or SIF as described above, 10 mL of digested MCFAs-containing liposomes solution was added to 10 mL of *n*-hexane and mixed well followed by centrifugation (8000 rpm) and extraction, to withdraw the unentrapped MCFAs. Then the entrapped MCFAs in liposomes were determined using a gas chromatograph (Agilent 6890 Series GC System, Agilent Technologies) following the method of Liu et al.[24] The cumulative amount of MCFAs released at different times was calculated using the equation

$$\text{\% release} = \frac{W_0 - W_t}{W_0} \times 100 \quad (4)$$

where W_0 is the value of MCFAs entrapped in liposomes at the beginning of digestion and W_t is the amount of MCFAs entrapped in liposomes at digestion time *t*.

dx.doi.org/10.1021/jf305329n | J. Agric. Food Chem. 2013, 61, 4133−4144

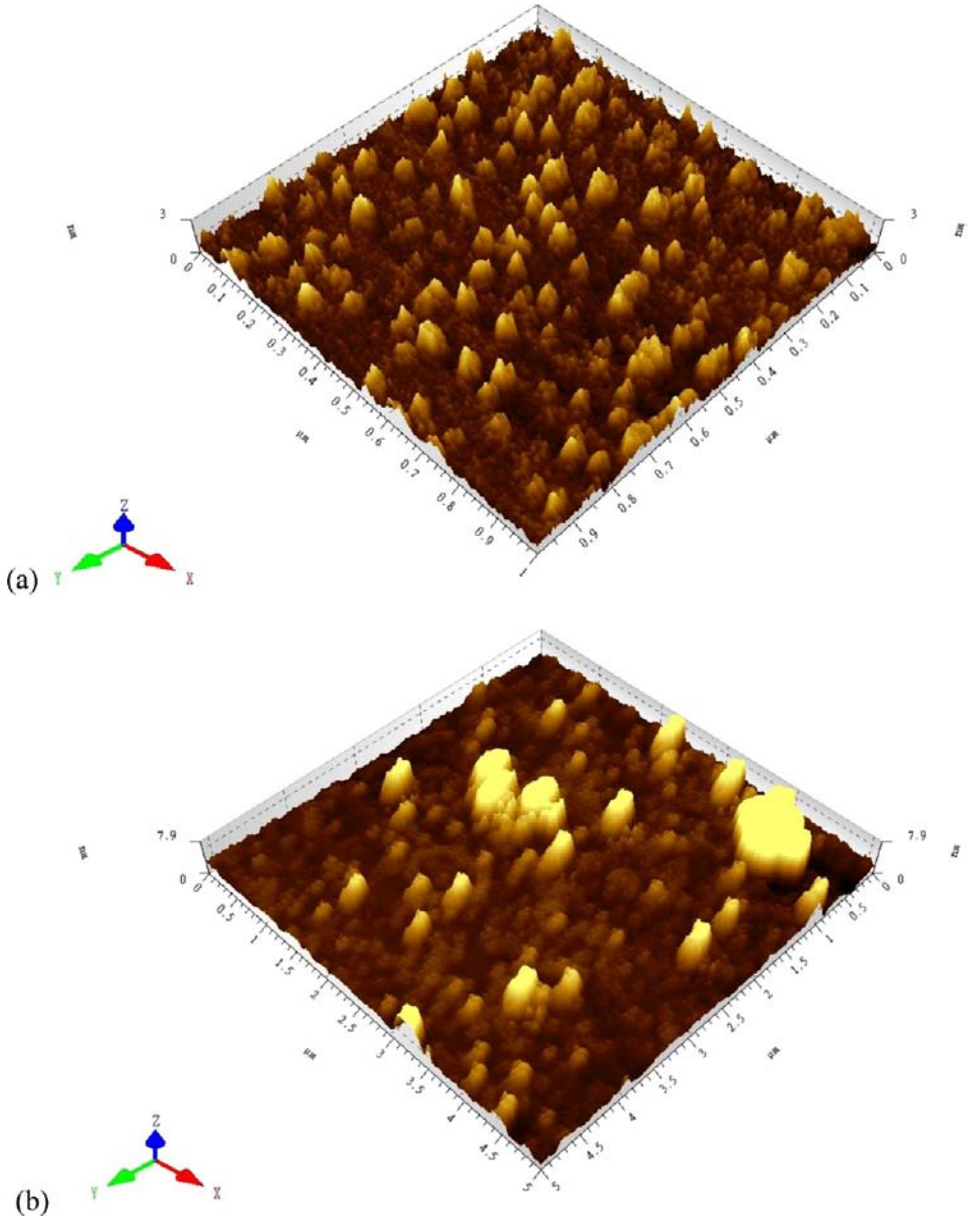

Figure 2. AFM images of nanoliposomes (a) and polyelectrolyte delivery system (b).

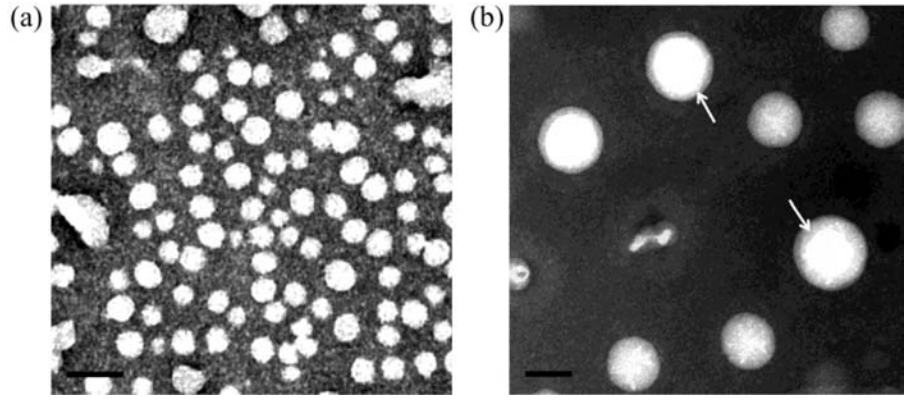

Figure 3. TEM images of nanoliposomes (a) and polyelectrolyte delivery system (b). Scale bar = 200 nm; arrows represent the core−shell structure.

Statistical Analysis. All measurements were replicated at least three times. The results were evaluated statistically for significance ($P \leq 0.05$) using analysis of variance and SPSS software version 18.0. All data were expressed as the mean ± standard deviation (SD).

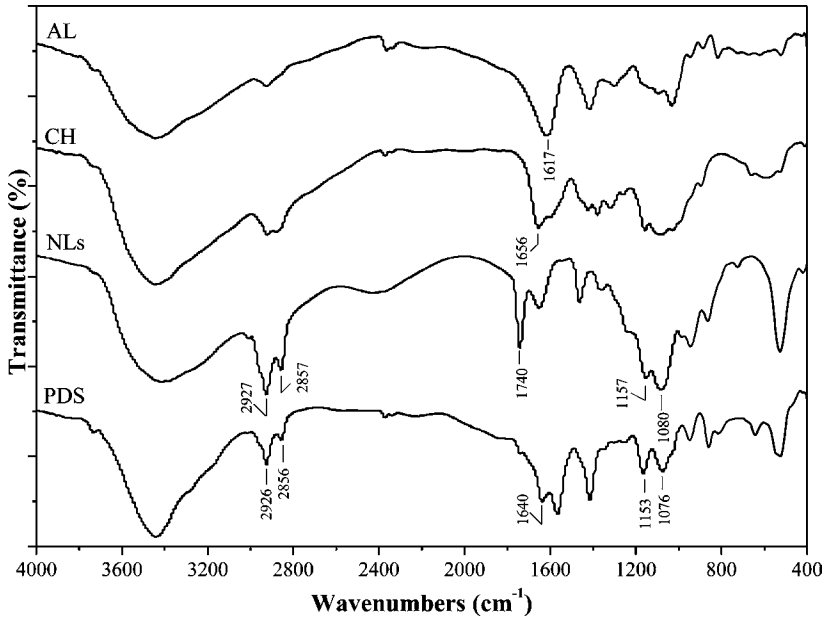

Figure 4. FTIR spectra of nanoliposomes (NLs) and polyelectrolyte delivery system (PDS) compared to chitosan (CH) and sodium alginate (AL).

RESULTS AND DISCUSSION

Characterization of PDS. As shown in Table 1, the average diameter and zeta potential of NLs were about 89 nm and −6.3 mV, respectively, with a PDI of 0.26. The concentrations of CH and AL played a significant role in the formulation of NLs. With the increase of CH concentration, the average diameter, zeta potential, and CH coating efficiency increased. A similar coating efficiency was obtained from the samples in the cases of 0.6% (65%) and 1% (66%) CH, however, liposomes coated with 1% of CH exhibited higher viscosity, and some flocculation could be found after storage for 48 h. Therefore, 0.6% of CH was selected as the first coating layer of NLs in the following experiments. On the other hand, when compared with the other concentrations of AL, the sample coated with 0.5% of AL displayed small particle size and low sedimentation efficiency. Hence, the appropriate concentration of AL for the following coating purpose was 0.5%. In contrast with NLs, the final formulation of AL−CH-coated NLs (PDS) was larger in average diameter (about 330 nm), with a PDI of 0.37, and the zeta potential exhibited a higher negative charge −15.8 mV at pH 5.5. According to Panya et al.,[34] the increase in particle size and negative charge of PDS could be due to the thicker interface of liposomes as well as bridging flocculation by the charged polymers.

To estimate whether NLs were coated with AL−CH and what the microstructure difference between NLs and PDS was, AFM and TEM photographs of both samples are demonstrated in Figures 2 and 3, respectively. According to the AFM micrographs, most of the NLs were well-distributed and PDS was less uniform, which was consistent with the profiles of multilayer nanocapsules as reported by Ye et al.[35] Besides, the average height of PDS was about 7.9 nm, which was equivalent to 2.7-fold of the NL thickness (3 nm). These representative images indicated that PDS yielded larger particle size (∼350 nm, Figure 2b) than NLs (∼80 nm, Figure 2a), and it coincided with the measurement by DLS. More details in coating were visualized in TEM (Figure 3). Without coating, NLs appeared as bright white spots and were spherical in shape (Figure 3a). After layering by AL and CH (Figure 3b), a core−shell structure can obviously be seen from the dark rim corresponding to the vesicle. Germain et al.[36] observed a similar microstructure in their liposomes coated with 25 cross-linked polyelectrolyte layers. They suggested that it may be ascribed to the fact that the polyelectrolyte prefers binding with stained molecules outside NLs. In our present study, the diameter measured by the two microscopes and the gray-white rim around the surface of NLs in TEM confirmed that the liposomal surface was generated by the deposition of polyelectrolyte.

The subtle changes in the structure of liposomes in the presence or absence of CH and AL observed by analyzing the frequency and the bandwidth alteration are shown in the FTIR spectra (Figure 4). The positions of symmetric and antisymmetric CH_2 stretching vibrations of the acryl chain (2857 and 2927 cm^{-1}, respectively) in NLs were hardly changed in the presence of AL and CH (2856 and 2926 cm^{-1}, respectively), whereas the carbonyl stretching vibration C═O of liposomal phospholipids decreased from 1740 cm^{-1} in NLs to 1640 cm^{-1} in PDS. The changes of signaling state C═O suggested a strengthening of the hydrogen bonds or even the formation of a new hydrogen bond in PDS.[37] In addition, the spectral pattern at 1080 and 1157 cm^{-1} represented the symmetric and antisymmetric PO_2^- stretching vibration of phospholipids, and the two peaks of PDS shifted to 1076 and 1153 cm^{-1}, respectively. The shift of the PO_2^- peak, which is sensitive to the formation of H-bonds, further indicated that there were hydrogen-bonding interactions between CH and NLs, and the coating was at the interfacial region of the bilayers.[38] Moreover, the characteristic peaks of the primary amino group of CH (1656 cm^{-1}) and the antisymmetric stretch at 1617 cm^{-1} (−COOH) of AL were not observable in PDS. It was revealed that the $-NH_3^+$ has reacted with the $-COO^-$,[39] which indicated AL had deposited on the surface of CH−NLs. These findings fit the data reported in the literature.[40] The spectral width of liposomes, for example, at 2927 cm^{-1}, decreased from 108 to 81 cm^{-1} for PDS. This implied a decrease in the membrane fluidity after surface modification, and thereby the stabilization of the polyelectrolyte system in

dx.doi.org/10.1021/jf305329n | J. Agric. Food Chem. 2013, 61, 4133−4144

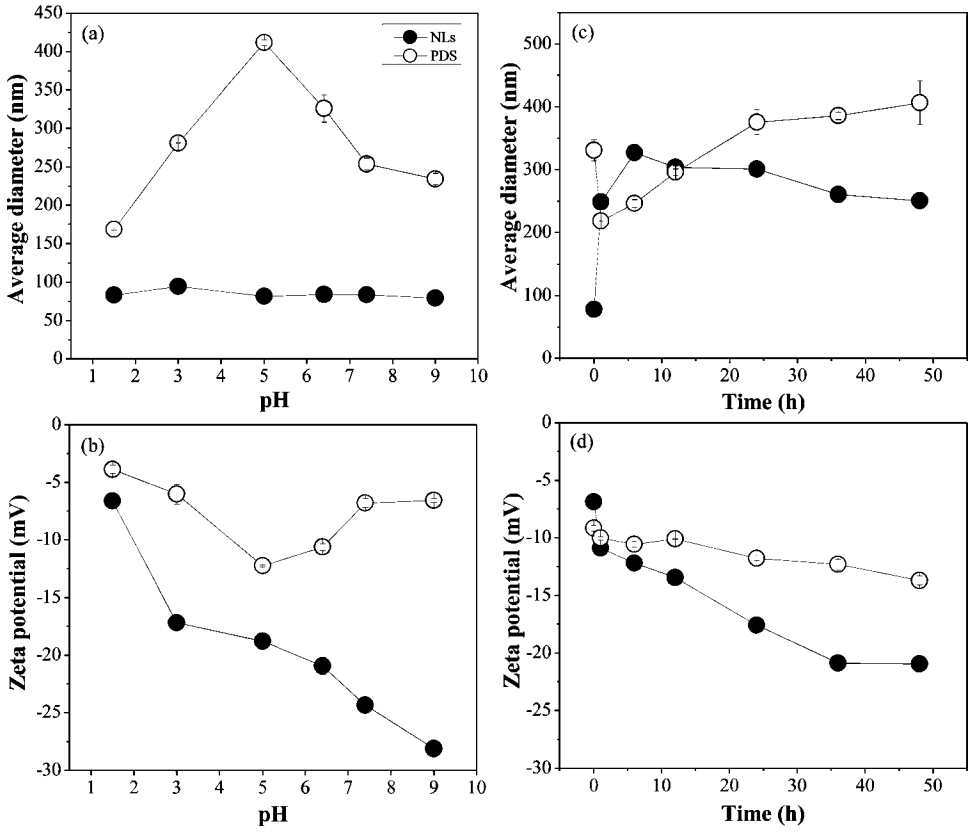

Figure 5. Effect of pH and heat treatment on average diameter and zeta potential of nanoliposomes (NLs) and polyelectrolyte delivery system (PDS): (a, c) changes in average diameter with pH and heat treatment time, respectively; (b, d) changes in zeta potential with pH and heat treatment time, respectively.

the gel phase improved.[41] FTIR results, which further supported the data obtained by DLS and the core−shell structure changes in TEM, demonstrated that AL and CH have been successfully coated on the surface of NLs.

Influence of pH on the Physical Stability of PDS. The changes in liposomal average diameter and zeta potential caused by pH adjustment are shown in Figure 5. The changes in average diameter of NLs were negligible (from 80 to 95 nm, Figure 5a). This was supported by our pervious study, which stated that the changes of pH could not damage liposomal structure.[30] For the changes of PDS, it was interesting to note that the particle size increased significantly from 170 nm at pH 1.5 to 410 nm at pH 5 and then decreased for the further increase of pH (235 nm at pH 9). This result suggested that although the particle size of PDS changed remarkably with the pH values, the cores (NLs) did not necessarily change (according to the results of NLs). The different trend between low-pH series and high-pH series can be mainly explained by the interaction between CH and AL under different pH conditions. AL has the property of shrinking in low pH and being dissolved in high pH, whereas CH dissolves in low pH and is insoluble in high pH ranges.[15] Therefore, at very low pH conditions (pH 1.5), outer-layer AL shrank and converted into an insoluble so-called alginic acid skin, which protected CH from dissolution.[42] As a result, PDS yielded the smallest size under the conditions and their cores were protected by AL networks. With pH value increase, AL networks became loose, and the media constantly entered the networks of CH and AL, leading to an increase in particle size. Our results were in agreement with Li et al.,[43] who obtained the smallest size of their AL−CH hydrogel beads at pH 1. However, they found that their diameter remarkably increased at pH 7 and the suspension was highly unstable to sedimentation at this condition. In our present study, however, there was a decrease in particle size when the pH was >5. It was known that the ionic interaction between CH and AL became weaker at high-pH conditions due to the dissolution of AL. Thus, it was supposed that the swelling of our particles was suppressed when the pH was >5, resulting in a gradual decrease in the average diameter of PDS. However, the inner layer of CH was insoluble and developed a loopier and globular conformation, which indicated the core was not easily affected by the environment.

The changes in profiles of NLs and PDS in zeta potential versus pH are shown in Figure 5b. As the pH increased, the negative surface charge of NLs decreased sharply (from −6.6 (pH 1.5) to −28.1 mV (pH 9)), probably because the electrostatic repulsion between particles became stronger with the pH increase. However, the negative surface charge of PDS decreased at the initial stages (from −3.9 (pH 1.5) to −12.3 mV (pH 5)) and then increased gradually (−6.6 mV at pH 9). The zeta potential of particles is sensitive to the surface compositions of the outermost layer. CH is positively charged when the pH is below its $pK_a \approx 6.5$ because of the charged amino groups ($-NH_3^+$), whereas higher pH causes its charge decrease ($-NH_2$). AL also exhibits a pH-sensitive behavior due to its carboxyl groups (−COOH), with an increase of negative charge at pH values greater than about 3.5 ($-COO^-$, $pK_a \approx 3.5$). Because many neutralized −COOH functional groups in AL were formed at very low pH, the zeta potential of PDS was

dx.doi.org/10.1021/jf305329n | J. Agric. Food Chem. 2013, 61, 4133−4144

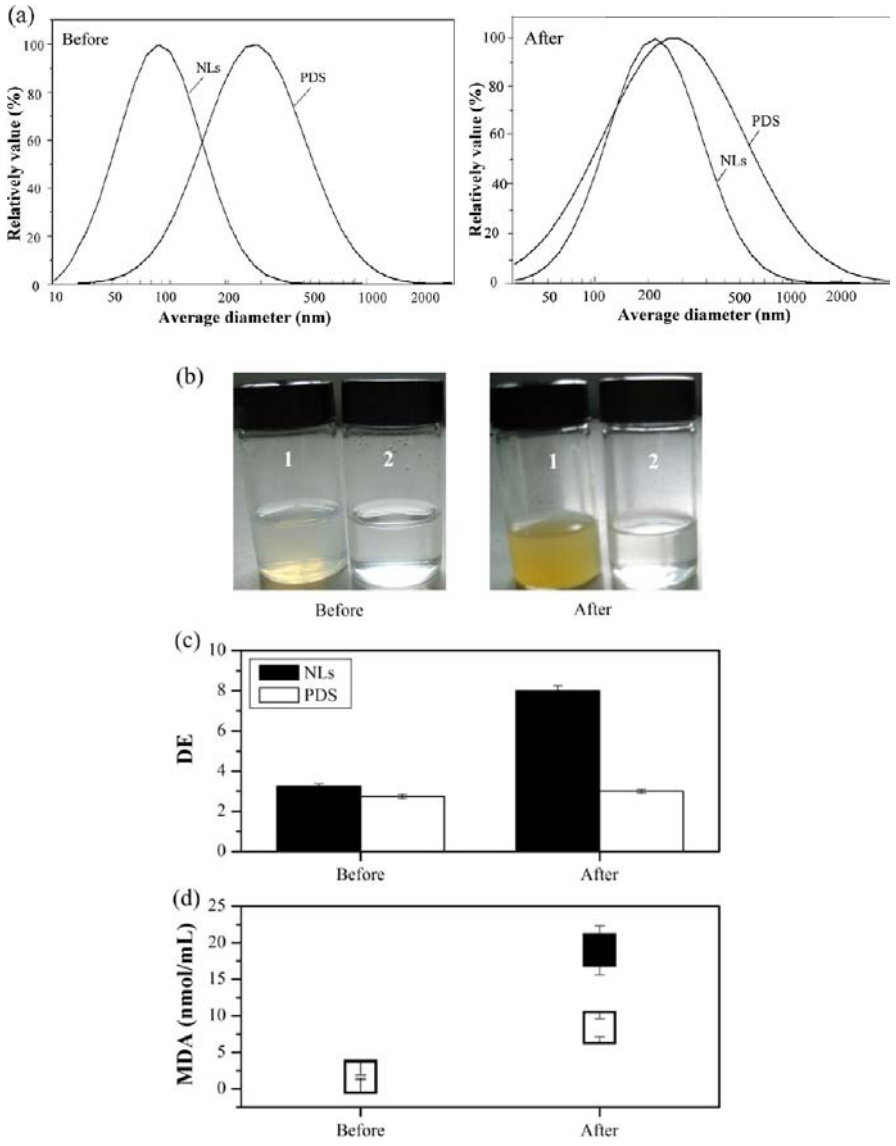

Figure 6. Changes in size distritution (a), appereance (b; 1, NLs; 2, PDS), color difference (c), and MDA (d) of nanoliposomes (NLs) and polyelectrolyte delivery system (PDS) before and after heat treatment.

close to zero. The decrease in negative charge with the increase of pH can be attributed to an increase of $-COO^-$ group of outer-layer AL. When the pH value was >5, the fact that PDS had less and less net negative surface charge suggested that AL was progressively dissolved and fewer protonated groups in CH were available for interaction.

In a word, the easy solubility of CH in low pH was prevented by the AL network because AL was insoluble in this condition, and the CH was stable at higher pH ranges, although AL might be dissolved.[15] As expected, the pH condition had an apparent influence on the average diameter and surface charge, but most of the changes were related to the outer-layer polymers. The cores (NLs) can be protected and maintained as an intact structure, and this would be further supported by the following experiments.

Influence of Heat Treatment on the Physical Stability of PDS. Heat treatment was an accelerated evaluation approach for the physical stability of liposomes. Very few studies have been published about the effect of heat treatment on the stability of modified liposomes. In the present study, the physical stability of PDS was also assessed by heat treatment under 70 °C water bath conditions for 48 h. As shown in Figure 5c, the average diameter of NLs remarkably increased at the initial 6 h heat treatment (from 78 to 304 nm). This result coincided with the study of Thompson et al.,[44] and it was suggested that there was an aggregation in the solution. A gradual decrease of particle size for the following heating time (250 nm, 48 h) might bring about partial degradation of liposomal membrane. For the sample of PDS, the average diameter decreased after heating for 1 h (from 330 to 218 nm), possibly owing to the degradation of outer-layer AL in high temperature. The following increase of particle size (406 nm, 48 h) was considered to be due to the increased propensity for interchain cross-linking of CH under the influence of heating.[45] Zeta potential analysis from sample surfaces clearly showed that the decrease of negative charges (absolute values increase) of NLs was sharper than that of PDS for 48 h of heating; that is, PDS changed from −9.2 to −13.7 mV, whereas NLs decreased from −6.9 to −20.9 mV (Figure 5d). These findings confirmed our understanding that the covered polymers act as colloidal

dx.doi.org/10.1021/jf305329n | J. Agric. Food Chem. 2013, 61, 4133−4144

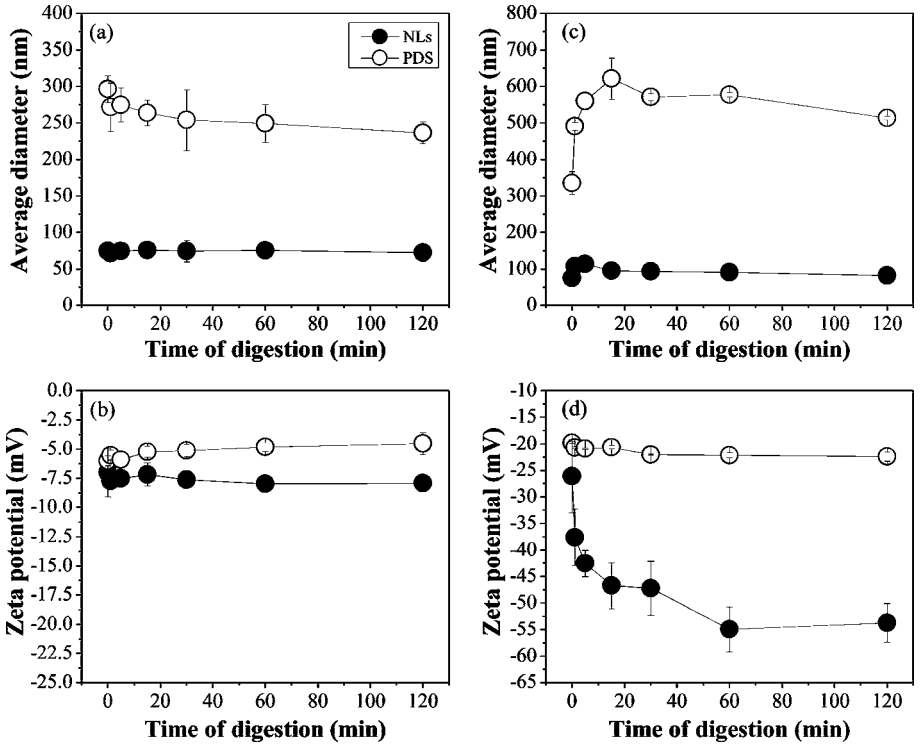

Figure 7. Digestion stability of nanoliposomes (NLs) and polyelectrolyte delivery system (PDS): (a, c) changes in average diameter of NLs and PDS during digestion in SGF and in SIF, respectively; (b, d) changes in zeta potential of NLs and PDS during digestion in SGF and in SIF, respectively.

protectors for NLs to some extent under high-temperature conditions.

More details about the effect of heat treatment on PDS are shown in Figure 6. Similar size distributions of NLs and PDS can be observed before heating, but the former displayed a narrower size distribution than the latter after 48 h of heating (Figure 6a). This was consistent with the changes that PDS displayed larger particle size after heating, compared with NLs. The visual appearance of the two samples was much different (Figure 6b). NLs (1) appeared to be light yellow and translucent before heating and became deeper and non-transparent after incubation for 48 h. On the contrary, almost no change in the appearance of PDS (2) was detected, with the solution consistently clear and transparent. Besides, lightness (L), redness (a), and yellowness (b) were determined for the color parameters and recorded in Figure 6c. A great difference in the color of NLs could be observed before and after heat treatment, with the DE values of 3.3 (easily noticeable, 3.0−6.0) and 8.0 (greatly noticeable, 6.0−12.0) CIELAB units, respectively. However, depending on the CD value of PDS, there was no significant difference between the nonheated (2.7 CIELAB units) and heated samples (3.0 CIELAB units) (noticeable, 1.5−3.0). Variations in color were in accordance with the visual appearance. Furthermore, the MDA value of NLs notably increased from 1.7 mmol/mL (before heating) to 19.0 mmol/mL (after heating for 48 h, Figure 6d). Nevertheless, the values of PDS were changed slightly (from 1.6 to 8.4 mmol/mL).

The uncoated NLs were changed apparently in appearance, color difference, and MDA (a final product of fatty acid peroxidation) after heating. These results are in agreement with Chandran et al.,[46] demonstrating that normal liposomes were thermolabile and that the lipids were likely to be hydrolyzed under high-temperature conditions. According to Heuvingh et al.,[47] the products of lipid peroxidation drastically affect the structural integrity of lipid vesicles due to the changes in the cross-section area of its lipid tails and solubility. However, slighter changes of AL−CH-coated NLs (PDS) in the parameters were observed. Although AL is known to degrade when it is subjected to heat treatment,[48] it was reported that CH underwent interchain cross-linking and this has been proposed to reduce lipid membrane fluidity.[45] Therefore, PDS were expected to have higher ability in resistance of high-temperature treatment than NLs.

Enzymic Digestion Stability of PDS. To determine the enzymic digestion stability of PDS in vitro, the average diameter and zeta potential were measured as a function of time (Figure 7). Liposomes without coating with AL and CH (NLs) were determined as a comparison. In SGF, the average diameters of both samples changed slightly during digestion with pepsin for 120 min (Figure 7a), and changes in the zeta potential of NLs and PDS were negligible as well (Figure 7b). Similar results were obtained in the study of Rowland and Woodley,[49] who reported that most liposomes were little affected by the low pH during passage through the stomach, and our previous study also confirmed this result.[30] The well-organized assembly of phospholipids can protect liposomes from gastric environment disintegration. Besides, the deposition of polymers on the surface of NLs may further be responsible for structure stabilization under low-pH conditions.

Different trends in particle size and zeta potential of both samples during digestion in SIF are also shown in Figure 7. Compared with NLs (from 107 to 114 nm), the particle size of PDS increased more significantly over the first 15 min of digestion (from 335 to 620 nm), and a gradual decrease thereafter was observed (530 nm at the end of digestion, Figure 7c). In SIF conditions (pH 7.4), there was a decrease in the number of charged cationic groups on the CH. Thus, the

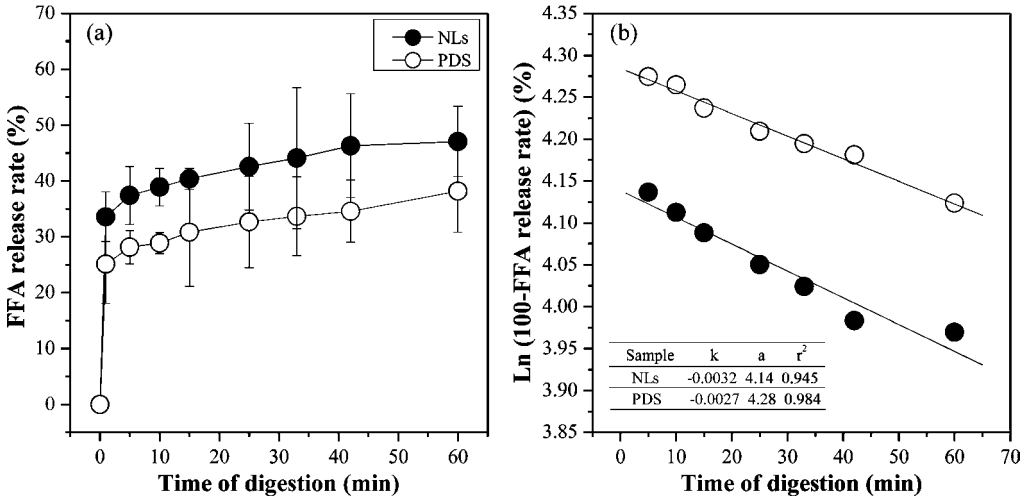

Figure 8. (a) Free fatty acid release of nanoliposomes (NLs) and polyelectrolyte delivery system (PDS) during digestion in SIF; (b) pseudo-first-order kinetic plots for NLs and PDS.

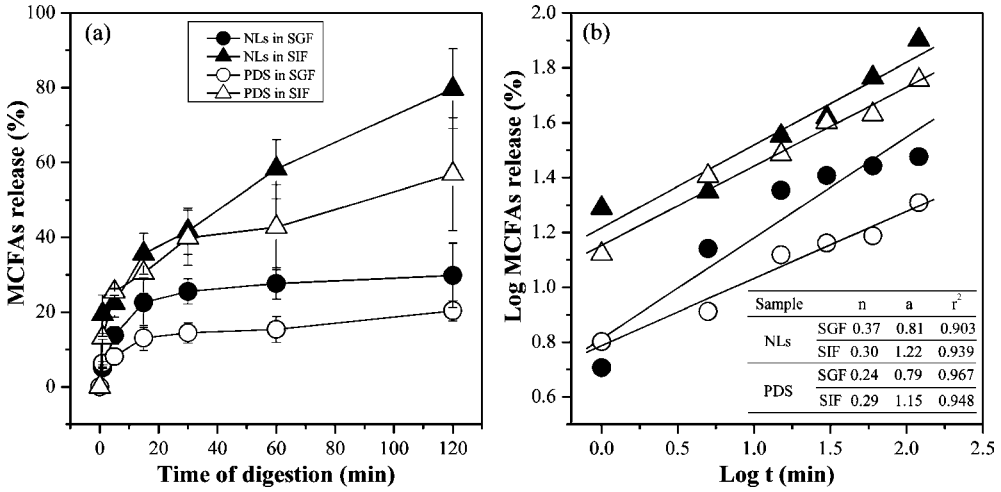

Figure 9. (a) Release profiles of MCFAs from nanoliposomes (NLs) and polyelectrolyte delivery system (PDS) during digestion in SGF and in SIF; (b) linear fits of the log of release data against log time.

electrostatic interaction between AL and CH was weaker, medium gradually entered into the particles, and average diameter increased. The subsequent decrease in average diameter of PDS during further digestion could be due to some of the AL being progressively dissolved, and the affinity of CH for ions in bile salts was higher than CH for liposomes.[50] For the surface charge, there was no significant change in the zeta potential of PDS during digestion in SIF for 120 min (from −20.1 to −22.4 mV, Figure 7d). However, the net negative charge of NLs increased for the whole digestion time (from −37.6 to −53.4 mV). The decrease of zeta potential of NLs may be attributed to the hydrolysis of phospholipids by pancreatin enzymes, whereas the smaller changes of PDS were probably caused by the protection of outer-layer polymers.

It was reported that the introduction of a polymer chain on the liposomal surface has often been performed to improve the dispersion stability and stiffness of the lipid layer.[51] Sometimes, however, adsorption of the polymer makes the coated particles aggregated (increase in size) or degraded (decrease in size) under specific conditions, such as at low- or high-pH environment in our present study (Figures 5a and 7c). These findings suggested that an enhanced AL-CH-coated liposome should be developed by some approach in future work, such as the use of a large-size liposome and thicker layers by repeated deposition.

Lipolysis Study. The release rate of FFA produced from the liposomal phospholipids was measured using pH-stat titration (Figure 8a). The lipid concentrations of NLs and PDS were 1.29 and 1.13 mg/mL, respectively. The digestion profiles of both samples exhibited similar trends, but the extent of lipid hydrolysis for PDS was lower than for NLs; that is, the FFA release rate of PDS (25%) was slower at the initial 1 min, followed by less lipid hydrolysis (38%) up to 60 min, compared to NLs (34 and 47%, respectively). In vivo, phospholipids are specifically catalyzed by lipase and phospholipase A_2, with concomitant liberated FFA and lysophospholipids.[52] Thus, the release of FFA is often taken to be a measure of liposomal stability. In our present results, the lower FFA release rate of PDS indicated that coated liposomes had a higher stability during the SIF digestion. Hu et al.[53] also found that coating of CH on the surface of lipid droplets could decrease the lipid digestion by pancreatin lipase. They predicted that it was CH that bind bile salts to resist their synergistic effect with phospholipiase A_2 on the hydrolysis of droplets. In our study,

dx.doi.org/10.1021/jf305329n | J. Agric. Food Chem. 2013, 61, 4133−4144

AL was used to coat the surface of CH-layered NLs. It was speculated that AL, together with CH, played a role in coverage blocking for liposomal hydrolysis. Both polymers may inhibit phospholipid digestion by restricting the ability of enzyme to reach the liposomal surfaces through a steric hindrance effect or specific binding effects.

A pseudo-first-order kinetic model was used to describe lipid degradation (eq 5).

$$\frac{F_t}{F_0} = e^{(-k/RT)} \tag{5}$$

where F_0 is the total amount of FFA released, F_t is the amount of FFA released at time t, k is the degradation rate constant for the pseudo-first-order model, R is the universal constant, and T is the absolute temperature. The fits and corresponding rate constants for lipolysis are shown in Figure 8b. The plot shows PDS had good linearity, which followed the model between 5 and 60 min with a reduction in lipid digestion rate constant. Similar results was reported in the study of Mohanraj et al.,[11] who demonstrated that liposomes covered with five layers of silica can reduce lipid lipolysis efficiently, and it fit the pseudo-first-order behavior well during intestinal digestion. Furthermore, PDS (−0.0027) yielded a smaller k value than NLs (−0.0032). It was further indicated that PDS had a better ability to resist lipolytic degradation by surface coverage blocking than NLs in SIF digestion.

In Vitro MCFAs Release Kinetics. MCFAs release profiles from NLs and PDS in SGF and SIF are presented in Figure 9a. At the initial 15 min of digestion in SGF, MCFAs released slowly from both of the samples (13.8% for NLs and 13.1% for PDS), and then there was negligible change of MCFAs release up to 120 min (29.8% for NLs and 20.4% for PDS). However, the release rate of PDS was slower than that of NLs over the whole digestion time. This might be responsible for the ability of AL to reduce the activity of pepsin and can be used to protect drugs from release at the acidity of gastric juice conditions.[54] Slow release of the contents in SGF was desirable for an oral delivery system, because there could be more MCFAs available for absorption in the intestine.

In contrast, the MCFAs release rate was more influenced in SIF than in SGF, and it was continuously increased up to 120 min (79.8% for NLs and 56.9% for PDS). These findings were consistent with our previous study, which stated that liposomes released more model-entrapped ingredient (calcein) in SIF than in SGF because of the disruption of liposomal membrane by pancreatic enzyme in SIF conditions.[30] In addition, it was clear that a delayed and reduced release rate of PDS compared with NLs was observed. Hermida et al.[55] and Lee et al.[56] have also found that normal liposomes lost their intact structure easily and thus released the entrapped materials under SIF conditions. In our present study, the reason for retarded release rate of PDS was attributed to the outer-layer polymers. Two possible mechanisms for this phenomenon were as follows: (a) there was a physical barrier (shrunkwn AL network at low pH and insoluble CH layers at high pH) formed on the surface of liposomes and then enzyme (pancreatic lipase, phospholipase A_2, and cholesterol esterase) was restricted to contact with liposomal phospholipids; (b) electrostatic bridges existing between the phospholipids and polymers reduced the permeability of the lipid bilayer.

To gain further insight into the MCFAs release mechanism, a drug release kinetics model was selected on the basis of the relevant correlation coefficients (r^2). Figure 9b shows the log MCFAs release rate from these vesicles as a function of log time. The data obtained were fit well to the Ritger−Peppas model in this study ($r^2 > 0.90$):[57]

$$\frac{R_t}{R_\infty} = at^n \tag{6}$$

R_t is the cumulative amount of MCFAs released in time t, R_∞ is the absolute cumulative amount of MCFAs released at infinite time (the value of MCFAs entrapped in liposomes at the beginning of digestion), a is the constant incorporating structural and geometrical characteristics of the dosage form, and n is the release exponent. According to Figure 9b, the n value of PDS (0.24 in SGF and 0.29 in SIF) was smaller than that of NLs (0.37 in SGF and 0.30 in SIF), but all of the release exponents were <0.5. For the sphere system, n has the limiting value of 0.50 in the case of Fickian diffusion.[57] Our results suggested that all of the samples were of Fickian diffusion process. In addition, the smaller n value of PDS can be explained as the larger particles had more steric hindrance caused by the coating of polymers on the liposomal surface. Zhu et al.[58] also reported this type of diffusion for gentamicin sulfate release from liposomes combined with β-TCP scaffold, and the rising particle size resulted in the decrease of the n value. The Ritger−Peppas model in our study suggested that PDS facilitated a low level of encapsulated material release in the simulated gastrointestinal tract.

This study has successfully prepared a PDS based on negatively charged AL and positively charged CH deposition on the surface of anionic NLs. The optimized formulation exhibited a core−shell structure in TEM and signal changes of characteristic peaks in FTIR. Physical stability studies, including analysis of surface charge, visual appearance, color difference, and malondialdehyde, suggested that polyelectrolyte can protect the core (NLs) from damage more efficiently and maintain PDS structure more intact than uncoated NLs. Furthermore, a quantitative estimate of in vitro enzymic digestion stability suggested that PDS could better prevent lipid degradation by the coverage blocking of outer-layer polymers and delayed release of encapsulated content, as compared with NLs. Thus, it was indicated that PDS could be developed as a promising delivery system for oral administration.

AUTHOR INFORMATION

Corresponding Author

*Phone: +86 791 88365872 (W.L.), +86 791 88305872 (C.L.). Fax: +86 791 88334509. E-mail: liuwei@ncu.edu.cn (W.L.), chengmeiliu@yahoo.com.cn (C.L.).

Funding

This research was supported by the National Natural Science Foundation of China (21266021), the Project of State Key Laboratory of Food Science and Technology, Nanchang University (No. SKLF-TS-201115), and the Jiangxi Province Postgraduate Innovation Fund (YC2011-B005).

Notes

The authors declare no competing financial interest.

REFERENCES

(1) Lasic, D.; Papahadjopoulos, D. Liposomes revisited. *Science (New York, NY)* **1995**, *267*, 1275.

(2) Min, B.; Cordray, J. C.; Ahn, D. U. Antioxidant effect of fractions from chicken breast and beef loin homogenates in phospholipid liposome systems. *Food Chem.* **2011**, *128*, 299−307.
(3) Aili, D.; Mager, M.; Roche, D.; Stevens, M. M. Hybrid nanoparticle−liposome detection of phospholipase activity. *Nano Lett.* **2010**, *11*, 1401−1405.
(4) da Silva Malheiros, P.; Daroit, D. J.; Brandelli, A. Food applications of liposome-encapsulated antimicrobial peptides. *Trends Food Sci. Technol.* **2010**, *21*, 284−292.
(5) Chiou, C.; Tseng, L.; Deng, M.; Jiang, P.; Tasi, S.; Chung, T.; Huang, Y.; Liu, D. Mucoadhesive liposomes for intranasal immunization with an avian influenza virus vaccine in chickens. *Biomaterials* **2009**, *30*, 5862−5868.
(6) Chun, J.; Choi, M.; Min, S.; Weiss, J. Mucoadhesive liposomes for intranasal immunization with an avian influenza virus vaccine in chickens. *Food Hydrocolloids* **2013**, *30*, 249−257.
(7) Reza Mozafari, M.; Johnson, C.; Hatziantoniou, S.; Demetzos, C. Nanoliposomes and their applications in food nanotechnology. *J. Liposome Res.* **2008**, *18*, 309−327.
(8) Zhang, L.; Granick, S. How to stabilize phospholipid liposomes (using nanoparticles). *Nano Lett.* **2006**, *6*, 694−698.
(9) Rameez, S.; Palmer, A. F. Simple method for preparing poly(ethylene glycol)-surface-conjugated liposome-encapsulated hemoglobins: physicochemical properties,long-term storage stability, and their reactions with O_2, CO, and NO. *Langmuir* **2011**, *27*, 8829−8840.
(10) Behera, T.; Swain, P.; Sahoo, S. K. Antigen in chitosan coated liposomes enhances immune responses through parenteral immunization. *Int. Immunopharmacol.* **2011**, *11*, 907−914.
(11) Mohanraj, V. J.; Barnes, T. J.; Prestidge, C. A. Silica nanoparticle coated liposomes: a new type of hybrid nanocapsule for proteins. *Int. J. Pharm.* **2010**, *392*, 285−293.
(12) Guo, X.; Wu, Z.; Guo, Z. New method for site-specific modification of liposomes with proteins using sortase a-mediated transpeptidation. *Bioconjugate Chem.* **2012**, *23*, 650−655.
(13) Qu, G.; Wu, X.; Yin, L.; Zhang, C. *N*-Octyl-*O*-sulfate chitosan-modified liposomes for delivery of docetaxel: preparation, characterization, and pharmacokinetics. *Biomed. Pharmacother.* **2012**, *66*, 46−51.
(14) Qiang, F.; Shin, H. L.; Lee, B. J.; Han, H. K. Enhanced systemic exposure of fexofenadine via the intranasal administration of chitosan-coated liposome. *Int. J. Pharm.* **2012**, *430*, 161−166.
(15) George, M.; Abraham, T. E. Polyionic hydrocolloids for the intestinal delivery of protein drugs: alginate and chitosan − a review. *J. Controlled Release* **2006**, *114*, 1−14.
(16) Jeon, O.; Alt, D. S.; Ahmed, S. M.; Alsberg, E. The effect of oxidation on the degradation of photocrosslinkable alginate hydrogels. *Biomaterials* **2012**, *33*, 3503−3514.
(17) Cheng, H. C.; Chang, C. Y.; Hsieh, F. I.; Yeh, J. J.; Chien, M. Y.; Pan, R. N.; Deng, M. C.; Liu, D. Z. Effects of tremella-alginate-liposome encapsulation on oral delivery of inactivated H5N3 vaccine. *J. Microencapsul.* **2011**, *28*, 55−61.
(18) Fujimoto, K.; Toyoda, T.; Fukui, Y. Preparation of bionanocapsules by the layer-by-layer deposition of polypeptides onto a liposome. *Macromolecules* **2007**, *40*, 5122−5128.
(19) Douglas, K. L.; Maryam, T. Effect of experimental parameters on the formation of alginate-chitosan nanoparticles and evaluation of their potential application as DNA carrier. *J. Biomater. Sci.* **2005**, *16*, 43−56.
(20) Ye, S.; Wang, C.; Liu, X.; Tong, Z. Deposition temperature effect on release rate of indomethacin microcrystals from microcapsules of layer-by-layer assembled chitosan and alginate multilayer films. *J. Controlled Release* **2005**, *106*, 319−328.
(21) Zhao, Q.; Han, B.; Wang, Z.; Gao, C.; Peng, C.; Shen, J. Hollow chitosan-alginate multilayer microcapsules as drug delivery vehicle: doxorubicin loading and in vitro and in vivo studies. *Nanomedicine* **2007**, *3*, 63−74.
(22) Haidar, Z. S.; Hamdy, R. C.; Tabrizian, M. Protein release kinetics for core−shell hybrid nanoparticles based on the layer-by-layer assembly of alginate and chitosan on liposomes. *Biomaterials* **2008**, *29*, 1207−1215.
(23) Liu, W. L.; Liu, W.; Liu, C. M.; Liu, J. H.; Zheng, H. J.; Yang, S. B.; Su, J. H. Preparation and evaluation of easy energy supply property of medium-chain fatty acids liposomes. *J. Microencapsul.* **2011**, *28*, 783−790.
(24) Liu, W.; Liu, W. L.; Liu, C. M.; Liu, J. H.; Yang, S. B.; Zheng, H. J.; Lei, H. W.; Ruan, R.; Li, T.; Tu, Z. C.; Song, X. Y. Medium-chain fatty acid nanoliposomes for easy energy supply. *Nutrition* **2011**, *27*, 700−706.
(25) Liu, W. L.; Liu, W.; Liu, C. M.; Yang, S. B.; Liu, J.; Zheng, H. J.; Su, K. M. Medium-chain fatty acid nanoliposomes suppress body fat accumulation in mice. *Br. J. Nutr.* **2011**, *106*, 1330−1336.
(26) Yang, S. B.; Liu, W.; Liu, C. M.; Liu, W. L.; Tong, G. H.; Zheng, H. J.; Zhou, W. Characterization and bioavailability of vitamin C nanoliposomes prepared by film evaporation-dynamic high pressure microfluidization. *J. Disper. Sci. Technol.* **2012**, *33*, 1608−1614.
(27) Liu, W.; Liu, J. H.; Xie, M. Y.; Liu, C. M.; Wan, J. Characterization and high-pressure microfluidization-induced activation of polyphenoloxidase from Chinese pear (*Pyrus pyrifolia* Nakai). *J. Agric. Food Chem.* **2009**, *57*, 5376−5380.
(28) Guo, J.; Ping, Q.; Jiang, G.; Huang, L.; Tong, Y. Chitosan-coated liposomes: characterization and interaction with leuprolide. *Int. J. Pharm.* **2003**, *260*, 167−173.
(29) Zhang, J.; Wang, S. Topical use of coenzyme Q10-loaded liposomes coated with trimethyl chitosan: tolerance, precorneal retention and anti-cataract effect. *Int. J. Pharm.* **2009**, *372*, 66−75.
(30) Liu, W. L.; Ye, A. Q.; Liu, C. M.; Liu, W.; Singh, H. Structure and integrity of liposomes prepared from milk- or soybean-derived phospholipids during in vitro digestion. *Food Res. Int.* **2012**, *48*, 499−506.
(31) Singh, H.; Sarkar, A. Behaviour of protein-stabilised emulsions under various physiological conditions. *Adv. Colloid Interface Sci.* **2011**, *165*, 47−57.
(32) Bonnaire, L.; Sandra, S.; Helgason, T.; Decker, E. A.; Weiss, J.; McClements, D. J. Influence of lipid physical state on the in vitro digestibility of emulsified lipids. *J. Agric. Food Chem.* **2008**, *56*, 3791−3797.
(33) Nakano, Y.; Mori, M.; Nishinohara, S.; Takita, Y.; Naito, S.; Kato, H.; Taneichi, M.; Komuro, K.; Uchida, T. Surface-linked liposomal antigen induces IgE-selective unresponsiveness regardless of the lipid components of liposome. *Bioconjugate Chem.* **2001**, *12*, 391−395.
(34) Panya, A.; Laguerre, M.; Lecomte, J.; Villeneuve, P.; Weiss, J.; McClements, D. J.; Decker, E. A. Effects of chitosan and rosmarinate esters on the physical and oxidative stability of liposomes. *J. Agric. Food Chem.* **2010**, *58*, 5679−5684.
(35) Ye, S.; Wang, C.; Liu, X.; Tong, Z. Multilayer nanocapsules of polysaccharide chitosan and alginate through layer-by-layer assembly directly on PS nanoparticles for release. *J. Biomater. Sci.−Polym. Ed.* **2005**, *16*, 909−923.
(36) Germain, M.; Grube, S.; Carriere, V.; Richard-Foy, H.; Winterhalter, M.; Fournier, D. Composite nanocapsules: lipid vesicles covered with several layers of crosslinked polyelectrolytes. *Adv. Mater.* **2006**, *18*, 2868−2871.
(37) Korkmaz, F.; Severcan, F. Effect of progesterone on DPPC membrane: evidence for lateral phase separation and inverse action in lipid dynamics. *Arch. Biochem. Biophys.* **2005**, *440*, 141−147.
(38) Bai, C.; Peng, H.; Xiong, H.; Liu, Y.; Zhao, L.; Xiao, X. Carboxymethylchitosan-coated proliposomes containing coix seed oil: characterisation, stability and in vitro release evaluation. *Food Chem.* **2011**, *129*, 1695−1702.
(39) Sankalia, M. G.; Mashru, R. C.; Sankalia, J. M.; Sutariya, V. B. Reversed chitosan−alginate polyelectrolyte complex for stability improvement of α-amylase: optimization and physicochemical characterization. *Eur. J. Pharm. Biopharm.* **2007**, *65*, 215−232.
(40) Mady, M. M.; Fathy, M. M.; Youssef, T.; Khalil, W. M. Biophysical characterization of gold nanoparticles-loaded liposomes. *Phys. Med.* **2012**, *28*, 288−295.

(41) Biruss, B.; Dietl, R.; Valenta, C. The influence of selected steroid hormones on the physicochemical behaviour of DPPC liposomes. *Chem. Phys. Lipids* **2007**, *148*, 84−90.
(42) Chen, S. C.; Wu, Y. C.; Mi, F. L.; Lin, Y. H.; Yu, L. C.; Sung, H. W. A novel pH-sensitive hydrogel composed of *N*,*O*-carboxymethyl chitosan and alginate cross-linked by genipin for protein drug delivery. *J. Controlled Release* **2004**, *96*, 285−300.
(43) Li, Y.; McClements, D. J. Controlling lipid digestion by encapsulation of protein-stabilized lipid droplets within alginate-chitosan complex coacervates. *Food Hydrocolloids* **2011**, *25*, 1025−1033.
(44) Thompson, A. K.; Haisman, D.; Singh, H. Physical stability of liposomes prepared from milk fat globule membrane and soya phospholipids. *J. Agric. Food Chem.* **2006**, *54*, 6390−6397.
(45) Wong, T. W.; Chan, L. W.; Kho, S. B.; Sia Heng, P. W. Design of controlled-release solid dosage forms of alginate and chitosan using microwave. *J. Controlled Release* **2002**, *84*, 99−114.
(46) Chandran, S.; Roy, A.; Mishra, B. Recent trends in drug delivery systems: liposomal drug delivery system − preparation and characterisation. *Indian J. Exp. Biol.* **1997**, *35*, 801−9.
(47) Heuvingh, J.; Bonneau, S. Asymmetric oxidation of giant vesicles triggers curvature-associated shape transition and permeabilization. *Biophys. J.* **2009**, *97*, 2904−2912.
(48) Draget, K. J. *Alginates*; Woodhead: Cambridge, UK, 2000; pp 379−395.
(49) Rowland, R. N.; Woodley, J. F. The stability of liposomes in vitro to pH, bile salts and pancreatic lipase. *Biochim. Biophys. Acta* **1980**, *620*, 400−409.
(50) Anal, A. K.; Bhopatkar, D.; Tokura, S.; Tamura, H.; Stevens, W. F. Chitosan-alginate multilayer beads for gastric passage and controlled intestinal release of protein. *Drug Dev. Ind. Pharm.* **2003**, *29*, 713−724.
(51) Maeda, T.; Fujimoto, K. A reduction-triggered delivery by a liposomal carrier possessing membrane-permeable ligands and a detachable coating. *Colloids Surf. B: Biointerfaces* **2006**, *49*, 15−21.
(52) Nishizuka, Y. Intracellular signaling by hydrolysis of phospholipids and activation of protein kinase C. *Science* **1992**, *258*, 607−614.
(53) Hu, M.; Li, Y.; Decker, E. A.; Xiao, H.; McClements, D. J. Influence of tripolyphosphate cross-linking on the physical stability and lipase digestibility of chitosan-coated lipid droplets. *J. Agric. Food Chem.* **2010**, *58*, 1283−1289.
(54) Tang, M.; Dettmar, P.; Batchelor, H. Bioadhesive oesophageal bandages: protection against acid and pepsin injury. *Int. J. Pharm.* **2005**, *292*, 169−177.
(55) Hermida, L. G.; Sabés-Xamaní, M.; Barnadas-Rodríguez, R. Combined strategies for liposome characterization during in vitro digestion. *J. Liposome Res.* **2009**, *19*, 207−219.
(56) Lee, J. S.; Kim, H. W.; Chung, D.; Lee, H. G. Catechin-loaded calcium pectinate microparticles reinforced with liposome and hydroxypropylmethylcellulose: optimization and in vivo antioxidant activity. *Food Hydrocolloids* **2009**, *23*, 2226−2233.
(57) Ritger, P. L.; Peppas, N. A. A simple equation for description of solute release I. Fickian and non-Fickian release from non-swellable devices in the form of slabs, spheres, cylinders or discs. *J. Controlled Release* **1987**, *5*, 23−36.
(58) Zhu, C. T.; Xu, Y. Q.; Shi, J.; Li, J.; Ding, J. Liposome combined porous *β*-TCP scaffold: preparation, characterization, and anti-biofilm activity. *Drug Deliv.* **2010**, *17*, 391−398.